

Pressure dependence of magnetism in URu₂Si₂

F. Bourdarot,¹ B. Fak,¹ V.P. Mineev,¹ M.E. Zhitomirsky,¹ N. Kernavanois,¹
S. Raymond,¹ P. Bulet,¹ F. Lapiere,² P. Lejay,² and J. Flouquet¹

¹DRFMC, SPSMS, CEA Grenoble, 38054 Grenoble, France

²Centre de Recherches sur les Très Basses Températures, CNRS, BP 166, 38042 Grenoble, France
(Dated: 29 August 2003; printed November 23, 2018)

Neutron-scattering and specific-heat measurements of the heavy-fermion superconductor URu₂Si₂ under hydrostatic pressure and with Rh-doping [U(Ru_{0.98}Rh_{0.02})₂Si₂] show the existence of two magnetic phase transitions. At the second-order phase transition $T_m \sim 17.5$ K, a tiny ordered moment is established, while at $T_M < T_m$, a first-order phase transition (under pressure or doping) gives rise to a large moment. The results can be understood in terms of a hidden OP ψ coupled to the ordered moment m , where m and ψ have the same symmetry.

PACS numbers: 75.25.+z, 75.30.Kz, 75.30.Cr, 75.50.Ee, 74.70.Tx

The phase transition at $T_m=17.5$ K in URu₂Si₂ is one of the most puzzling features in heavy-fermion systems. Most bulk properties display anomalies at T_m , and in particular there is a huge jump of $\Delta C/T_m=0.3$ JK⁻²mol⁻¹ in the specific heat [1]. These anomalies cannot be explained by the tiny ordered moment of $\sim 0.03 \mu_B$, which also develops at T_m . The antiferromagnetic (AFM) structure, observed both by neutron [2, 3, 4, 5, 6, 7] and x-ray [8] scattering, is characterized by a propagation vector $\mathbf{k}=(001)$ and dipolar moments along the c axis of the body-centered tetragonal structure (I4/mmm).

In a recent *tour de force* experiment combining neutron elastic scattering with high magnetic fields [7], it was found that the magnetic moment in URu₂Si₂ did not disappear at 15 T as suggested by the extrapolation of earlier low-field data [5, 6], but remains finite at 17 T with an inflection point near 7 T. The particular field dependence of the ordered moment, $m(H)$, agrees with the predictions of a model containing two order parameters (OPs) with the same symmetry [9], based on the theoretical work of Ref. [10].

In this Letter, we present new experimental data where hydrostatic or chemical pressure is used to tune the interactions in the system. The main result is the existence of two distinct phases in the p - T phase diagram of URu₂Si₂ for pressures $p > p_M$, where $p_M \approx 4.9$ kbar (see Fig. 1), or for small Rh doping. The existence of two phases have also been inferred from thermal expansion measurements [11], but, as will be discussed later, their phase diagram is fundamentally different from ours. We call the two magnetic phases for small-moment (SMAF) and large-moment (LMAF) antiferromagnetic phases. The SMAF phase, observed below the second-order phase transition at $T_m \approx 17.5$ K ($T_m(p)$ in Fig. 1 is determined from resistivity measurements under pressure, Ref. [12]), is the same as that observed at $p=0$ and is characterized by a small moment m and large anomalies in the macroscopic properties. The low-T LMAF phase, observed below the transition T_M , which seems to be a first-order transition, is characterized by a large moment m and small

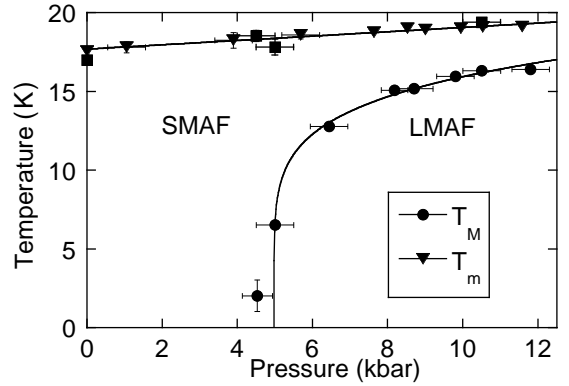


FIG. 1: Pressure-temperature phase diagram of URu₂Si₂ showing the SMAF and LMAF phases determined from neutron scattering (circles and squares) and resistivity measurements (triangles, Ref. [12]). The lines are guides to the eye.

anomalies in the macroscopic properties. The SMAF and LMAF phases have the same magnetic structures.

Many phenomenological theories for URu₂Si₂ introduce two physical quantities or “order parameters”: an AFM parameter m that describes ordering of localized dipolar $5f$ moments and a hidden (unknown) order ψ responsible for the $T_m=17.5$ K transition [9, 10]. It has been suggested that ψ could originate from triple-spin correlators of $5f$ electrons [10] or an exotic spin-density wave. The Landau free energy for the two OP’s (up to fourth-order terms) can be written as

$$F = \alpha_\psi \psi^2 + \alpha_m m^2 + 2\gamma \psi m + \beta_\psi \psi^4 + \beta_m m^4 + 2\beta_i \psi^2 m^2 \quad (1)$$

The coupling term ψm is allowed only if m and ψ transform according to the same irreducible representation, otherwise $\gamma \equiv 0$. Coupling terms of type $\psi^3 m$ and ψm^3 can be removed from Eq. (1) by linear transformation. Shah *et al.* [9] studied the above free energy at zero pressure and finite magnetic fields H and predicted an inflection point for $m(H)$ only in the case $\gamma \neq 0$. This was

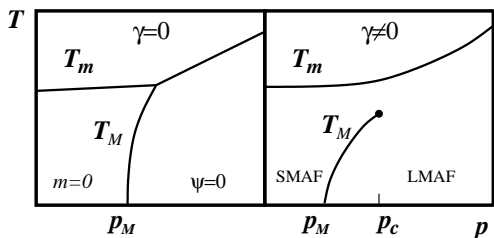


FIG. 2: Schematic phase diagram for the 2OP functional Eq. (1) for $\gamma=0$ (left panel) and $\gamma \neq 0$ (right panel).

recently observed experimentally [7]. Motivated by this agreement, we investigate here the functional Eq. (1) as a function of pressure.

For $\gamma \neq 0$, the two OP's appear simultaneously below the transition line from the paramagnetic state $T_m(p)$, given by $\alpha_\psi \alpha_m = \gamma^2$. At $p=0$, the AFM OP behaves as $m \approx -(\gamma/\alpha_m)\psi$ (for $|\alpha_\psi|, |\gamma| \ll \alpha_m$). A small coefficient γ/α_m implies weak ordered moments, while ψ gives rise to a large anomaly in the specific heat at T_m , as in the SMAF phase. The presence and nature of extra transitions below $T_m(p)$ depend on quartic terms in Eq. (1). Since the transition at T_M appears to be first order, we consider the case $\beta_i > \sqrt{\beta_\psi \beta_m}$.

The p - T phase diagram for $\gamma=0$ is sketched in the left panel of Fig. 2. The line of first-order phase transitions $T_M(p)$ between states with $m=0$ and $\psi=0$ emerges from the kink point on $T_m(p)$. The equation for $T_M(p)$ is $\alpha_\psi^2 \beta_m = \alpha_m^2 \beta_\psi$. Such a phase diagram was recently considered by Chandra *et al.* [13] in their interpretation of small AFM moments as a phase separation effect.

The recently observed inflection point in $m(H)$ [7], however, points to an intrinsic origin of the tiny ordered moment and a finite γ . For $\gamma \neq 0$, the first-order transition line $T_M(p)$ is stable and its position in the p - T plane is given by the same equation as for $\gamma=0$. However, $T_M(p)$ splits from the line of second order transitions $T_m(p)$ and terminates at a critical point p_c below T_m (right panel of Fig. 2). The location of the critical point is given by $\alpha_\psi^c = -2|\gamma|(\beta_\psi^3 \beta_m)^{1/4}/(\beta_i - \sqrt{\beta_\psi \beta_m})$. The two states above and below $T_M(p)$ are phases with large ψ_L and small m_S (SMAF) and with small ψ_S and large m_L (LMAF), respectively. A relative jump of the ordered AFM moments across $T_M(p)$ is given by $(m_L - m_S)/(m_L + m_S) = \sqrt{(\alpha_\psi - \alpha_\psi^c)/(\alpha_\psi + \alpha_\psi^c)}$. The size of the jump varies continuously along $T_M(p)$ and vanishes at $p = p_c$. The corresponding phase diagram, shown schematically in the right panel of Fig. 2, resembles the vapor-liquid phase diagram.

The first evidence for the existence of two phase transitions were obtained from neutron scattering and specific-heat measurements on a Rh doped sample: $\text{U}(\text{Ru}_{0.98}\text{Rh}_{0.02})_2\text{Si}_2$ [14]. The T dependence of the ordered magnetic moment (see inset of Fig. 3) clearly shows

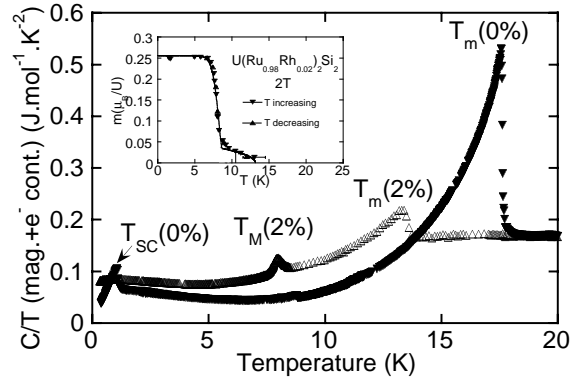


FIG. 3: Electronic specific heat (after subtraction of the phonon contribution obtained from ThRu_2Si_2) divided by temperature for URu_2Si_2 and for $\text{U}(\text{Ru}_{0.98}\text{Rh}_{0.02})_2\text{Si}_2$. The inset shows the T dependence of the magnetic moment in $\text{U}(\text{Ru}_{0.98}\text{Rh}_{0.02})_2\text{Si}_2$ for decreasing and increasing T .

two transitions at $T_M=8.3$ K and $T_m=13.2$ K, with saturation moments (extrapolated to $T \rightarrow 0$) of 0.25 and 0.04 μ_B , respectively. The transition at T_M has a first order shape (although no hysteresis was observed) while that at T_m is second order. These measurements were performed on the DN3 neutron diffractometer at the Siloé reactor using a wavelength of 1.54 Å and on the thermal triple-axis spectrometer 2T at the Orphée reactor with a final wave vector $k_f = 2.662 \text{ \AA}^{-1}$ on a 1.2 g annealed Czochralski-grown single crystal of $\text{U}(\text{Ru}_{0.98}\text{Rh}_{0.02})_2\text{Si}_2$.

Specific heat measurements (see Fig. 3) show that while the large jump in the specific heat is associated with a small moment, the small jump is associated with a large moment estimated at 0.16 μ_B [15]. This shows that while there is no relation between the small moment m_S and $\Delta C/T_m$, the large moment m_L is consistent with the specific heat anomaly at T_M . The entropy jump of the LMAF transition deduced from these measurements corresponds to $\Delta S(T_M) = 23 \text{ mJ.K}^{-1}\text{mol}^{-1}$. The effect of Rh doping is more subtle than a simple (negative) pressure, since Rh is not isoelectronic with Ru. The added electron modifies the band structure, and while the volume increases slightly, the low- T lattice parameter a decreases and c increases, as shown by X-ray measurements on the ID31 beam line at the ESRF [16]. Using the Clausius-Clapeyron relation with ΔV deduced from the pure URu_2Si_2 [11], a large slope dT_M/dp is found, characteristic of a first-order phase transition.

Experiments under hydrostatic pressure on the pure compound show strong similarities with the Rh-doped sample. Neutron-scattering measurements were performed at the Institut Laue-Langevin (ILL) on the D15 diffractometer using a wavelength of 0.85 Å and on the IN22 triple-axis spectrometer using a final wave vector

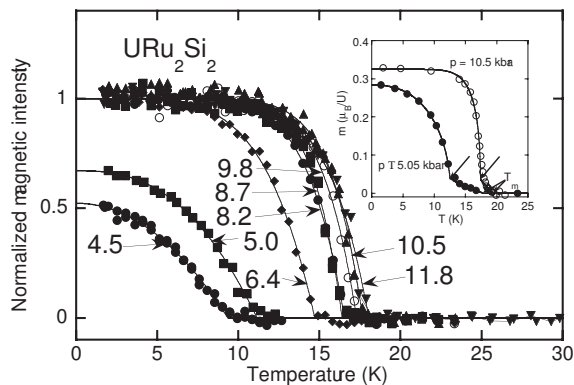


FIG. 4: Normalized intensity ($\propto m^2$) of the ordered magnetic moment in URu_2Si_2 as a function of increasing temperature for different pressures. The pressures 8.7, 10.5, and 11.8 were also measured for decreasing temperature. The inset shows the temperature dependence of the magnetic moment m at $p=5.05$ kbar and 10.5 kbar with the two transitions. The arrows show the onset of the LMAF phase.

of 2.662 \AA^{-1} . A 4.8-mm diameter crystal was cut from the same batch used in the high-field measurements of Ref. [7] with the a axis along the 4-mm long cylinder axis. Standard ILL CuBe and steel clamp pressure cells of inner diameter of 5 or 6 mm were used for most measurement with fluorinert as pressure transmitter. Complementary measurements were made with an ILL He-gas pressure cell. On D15, the pressure was determined from the lattice spacing of a NaCl crystal mounted inside the pressure cells.

The observed temperature dependence of the magnetic intensity ($\propto m^2$) of URu_2Si_2 is shown in Fig. 4 for different pressures. The increase of the temperature slope, $dm^2(T)/dT$, with pressure near T_M indicates that the phase transition is first order. This behavior is opposite to that expected for a pressure gradient if the transition is second order, and is thus an intrinsic effect. Fitting the expression $m^2 = m_0^2[1 - (T/T_M)^\alpha]$ [4] leads to $\alpha \leq 2.5$ for pressures below 5 kbar, while a much larger value, $\alpha \sim 8.5$, is obtained at higher pressures, suggestive of a first order transition. The phase diagram presented in Fig. 1 is constructed from the data shown in Fig. 4, where T_M is taken as the *midpoint* of the transition, which is the correct estimate for a first-order transition in the presence of pressure gradients. The presence of pressure gradients, usually estimated to $\Delta p/p \sim 5\%$ for the used clamp cells, is clear from the strong intensity observed at 4.5 kbar using a clamp cell (Fig. 4), since measurements in a He-gas pressure cell at $p = 4.45 \pm 0.15$ kbar show no (large) ordered moment on D15, where the detection limit is $0.06 \mu_B$. We also note that the magnetic intensity saturates at a value of $0.33 \mu_B$ for pressures $p \geq 6.4$ kbar. The critical pressure for the onset of the large moment is es-

timated to $p_M = 4.9 \pm 0.2$ kbar. As for the doped Rh sample (see inset of Fig. 3), no hysteresis was observed in $m^2(T)$. However, the vertical slope of dT/dp in Fig. 1 is a strong evidence of a first-order transition. The absence of magnetic scattering at the $(0,0,2l+1)$ reflections shows that the ordered moments are along the c -axis at all pressures, i.e. the SMAF and LMAF phases have the same AFM structure. We finally note that while the AFM Bragg peaks are resolution limited in the LMAF phase [16, 17], they have a finite correlation length of a few hundred \AA in the SMAF phase [2, 4, 16, 17].

The longitudinally polarized magnetic excitations were studied under pressure on IN22 at the two wave vectors $\mathbf{Q}_1=(1,0,0)$ and $\mathbf{Q}_2=(1.4,0,0)$, which correspond to the minima in the $p=0$ dispersion curve of URu_2Si_2 [2]. Spectra for energy transfers up to 7 meV were performed with $k_f=1.55 \text{ \AA}^{-1}$ and a 5-cm long Be filter in the scattered beam to reduce higher-order contamination; the energy resolution was 0.3 meV. Complementary spectra for energy transfers up to 16 meV were performed with $k_f=2.662 \text{ \AA}^{-1}$ and a 4-cm long pyrolytic graphite filter in the scattered beam; the energy resolution was 0.9 meV.

The measurements show pronounced differences in the excitation spectra between the LMAF and SMAF phase. In the SMAF phase, $T_M < T < T_m$, the two excitations at a finite pressures of 5.0 kbar are very similar to those at zero pressure, with the same gap energies of $\Delta_1=1.6$ and $\Delta_2=4.5$ meV at \mathbf{Q}_1 and \mathbf{Q}_2 , respectively [see Figs. 5(a-b)]. In the LMAF phase, however, the excitation at \mathbf{Q}_1 is absent [see Fig. 5(c)]. There is no clear feature at this wave vector in the measured spectra for energy transfers between 1 and 16 meV, in agreement with Ref. [18]. This suggests that the \mathbf{Q}_1 excitation is closely related to ψ , which is small in the LMAF phase. The excitation at \mathbf{Q}_2 , on the other hand, is readily seen. Its energy depends on pressure: we found $\Delta_2=7.7, 8.6,$ and 9.2 meV at pressures of 5, 9, and 10.5 kbar, respectively.

Our neutron scattering measurements on the 2% Rh-doped sample reveal that the excitations (not shown) are very similar to the pure compound under pressure. In the SMAF phase, the excitations at both \mathbf{Q}_1 and \mathbf{Q}_2 are present. In the LMAF phase, the excitation at \mathbf{Q}_1 is absent, as in URu_2Si_2 under pressure, while the excitation at \mathbf{Q}_2 is still present.

We will now discuss our results in the context of other work. Recent thermal-expansion measurements also observe a first-order transition under pressure [11]. The authors construct a phase diagram where the first-order transition line appears to join the second-order line around a pressure of 11 kbar. This would imply that the coefficient γ in Eq. (1) is zero, in clear contradiction with high-field measurements [7]. Our data, cf. Fig. 1, clearly show that the first and second order lines are nearly parallel at these pressures, and the most likely scenario is that the first-order line has an endpoint (cf. right panel of Fig. 2), and hence $\gamma \neq 0$.

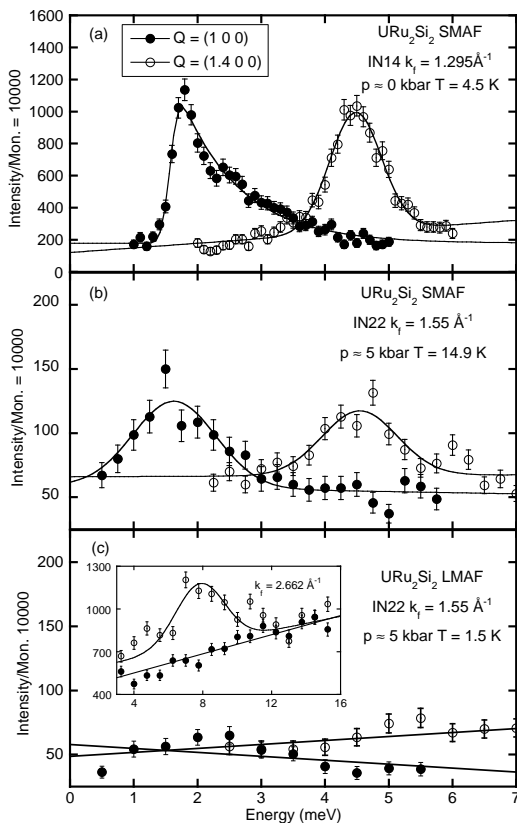


FIG. 5: Intensity *vs.* energy transfer for $\mathbf{Q}_1=(1,0,0)$ and $\mathbf{Q}_2=(1.4,0,0)$. (a) SMAF phase at $p=0$ and $T < 5$ K shows two well-defined excitations at \mathbf{Q}_1 and \mathbf{Q}_2 . (b) SMAF phase at $p=5$ kbar and $T > 7$ K also shows two well-defined excitations (the apparent broadening of the peaks is due to a coarser resolution and a higher T for this measurement). (c) LMAF phase at $p=5$ kbar and $T=1.5$ K shows the absence of the \mathbf{Q}_1 excitation and a strongly increased energy of the \mathbf{Q}_2 excitation (inset).

NMR [19] and μ SR [20] measurements have also observed a large moment under pressure, i.e. in the LMAF phase. The coexistence of an AFM signal with a “paramagnetic” signal in the NMR measurements under pressure and a magnetic field of a few Tesla on an aligned but crushed powder sample by Matsuda *et al.* [19] was interpreted in terms of a spatially inhomogeneous AFM ordering. There are several arguments against such a scenario. First, it would be a curious coincident if the AFM and the hidden order would have the same transition temperature in a phase-separated scenario, since m and ψ are not coupled as they occur in different parts of the sample. Secondly, one would not expect the \mathbf{Q}_1 excitation to disappear at a pressure where the two phases still coexist, just a smooth intensity change as the population of the two phases changes with pressure. Thirdly, a phase-separated scenario is inconsistent with a num-

ber of other experiments, such as the recent de Haas-van Alphen measurements under pressure [21] and the NMR measurements by Bernal *et al.* [22]. Since the temperature dependence observed in Ref. [19] is suggestive of either a large pressure gradient or strong internal strains, it would be important to repeat ²⁹Si-NMR measurements under pressure on a well-characterized single crystal. We recall here that the magnetism of URu₂Si₂ is very sensitive to the sample quality [4]. Indeed, the neutron scattering measurement under pressure on an annealed but otherwise uncharacterized crystal (closely related to that of Ref. [19]) presented in Ref. [17] are partly inconsistent with our neutron scattering experiments, the thermal-expansion measurements of Ref. [11], and their own μ SR work [20].

In conclusion, both the p - T phase diagram (this work) and the magnetic-field dependence of the ordered moment [7] in URu₂Si₂ are in excellent agreement with a scenario where a hidden OP is linearly coupled to the ordered moment and hence breaks time-reversal symmetry.

We acknowledge discussions with M.B. Walker and I. Fomin and experimental support from A.A. Menovsky, A.D. Huxley, E. Ressouche, J.L. Laborier, F. Fauth, L. Paolasini, A. Bombardi, F. Yakhov and N. Pyka. We thank G. Motoyama and N.K. Sato for sending us complementary thermal expansion data.

-
- [1] T.T.M. Palstra *et al.*, Phys. Rev. Lett. **55**, 2727 (1985).
 - [2] C. Broholm *et al.*, Phys. Rev. Lett. **58**, 1467 (1987); C. Broholm *et al.*, Phys. Rev. B **43**, 12 809 (1991).
 - [3] M.B. Walker *et al.*, Phys. Rev. Lett. **71**, 2630 (1993).
 - [4] B. Fåk *et al.*, J. Magn. Magn. Mater. **154**, 339 (1996).
 - [5] T.E. Mason *et al.*, J. Phys. Cond. Matter **7**, 5089 (1995).
 - [6] P. Santini *et al.*, Phys. Rev. Lett. **85**, 654 (2000).
 - [7] F. Bourdarot *et al.*, Phys. Rev. Lett. **90** 067203, (2003).
 - [8] E.D. Isaacs *et al.*, Phys. Rev. Lett. **65**, 3185 (1990).
 - [9] N. Shah *et al.*, Phys. Rev. B **61**, 564 (2000).
 - [10] D. F. Agterberg and M. B. Walker, Phys. Rev. B **50**, 563 (1994).
 - [11] G. Motoyama *et al.*, Phys. Rev. Lett. **90**, 166402 (2003).
 - [12] L. Schmidt, Ph. D. Thesis, UJF Grenoble (1993).
 - [13] P. Chandra *et al.*, Physica B **312-313**, 397 (2002).
 - [14] F. Bourdarot, Ph. D. Thesis, UJF Grenoble (1994).
 - [15] The moment was estimated from the AFM energy in molecular field theory: $(m_0/m_{sat})^2 = (2/3k_B T_N) \int_0^{T_N} C_{mag}(T) dT$, with $m_{sat} = 3.62\mu_B$.
 - [16] F. Bourdarot *et al.*, unpublished x-ray work.
 - [17] H. Amitsuka *et al.*, Phys. Rev. Lett. **83**, 5114 (1999).
 - [18] N. Metoki *et al.*, Physica B **280**, 362 (2000)
 - [19] K. Matsuda *et al.*, Phys. Rev. Lett. **87**, 087203 (2001).
 - [20] H. Amitsuka *et al.*, Physica B **326**, 418 (2003).
 - [21] M. Nakashima *et al.*, Physica B, in press.
 - [22] O.O. Bernal *et al.*, Phys. Rev. Lett. **87**, 196402 (2001).